Radiation Absorbed Dose from Indium-111-CYT-356

G. Mardirossian, A.B. Brill, K.M. Dwyer, D. Kahn and W. Nelp

University of Massachusetts Medical Center, Nuclear Medicine Department, Worcester, Massachusetts; Cytogen Corporation, Princeton, New Jersey; University of Iowa College of Medicine and Iowa City Veterans Affairs Medical Center, Iowa City, Iowa; and University of Washington Medical Center, Radiology Department, Seattle, Washington

Indium-CYT-356 is an agent developed by CYTOGEN Inc. (CYT) (Princeton, NJ) for the use in staging patients with prostate cancer. This investigation was performed to provide the human dosimetry needed for Food and Drug Administration approval for routine use in patients. **Methods:** Biodistribution data collected from three sites were obtained from prostate cancer patients who received diagnostic doses of ^{111}In-CYT-356. Data included blood and urine collections, and the organ uptake value was measured from sequential conjugate whole-body and planar images over a 7–10 day period. Dose contributions from radioactivity in transit through the GI tract were estimated using a compartmental model. The calculations used the MIRD methodology and MIRDOSE 3. **Results:** The total-body dose observed was 0.14 mGy/MBq, and the effective dose was found to be 0.25–0.29 mSv/MBq. The largest organ doses were found for the liver (1.0 mGy/MBq), kidneys (0.67 mGy/MBq) and spleen (0.88 mGy/MBq). **Conclusion:** The radiation dose to the patient from a typical 185 MBq administration of ^{111}In-CYT-356 is comparable to the dose from other ^{111}In-labeled whole antibodies used in the diagnosis and management of cancer patients. The inclusion of the GI tract as a source organ increases the effective dose by 18%.

Key Words: dosimetry; monoclonal antibodies; prostate cancer

J Nucl Med 1996; 37:1583–1588

Monoclonal antibodies labeled with a variety of radionuclides, primarily ^{111}In and ^{99m}Tc are in routine diagnostic use in much of the world. The first approved radioimmunodiagnostic agent in the United States, OncoScint CR/OV, was approved by the Food and Drug administration (FDA) in December 1992 for routine use in patients with colorectal and ovarian cancer. CYT 356, also known as Capromab Pendetide, is an ^{111}In-labeled IgG antibody against a prostate specific membrane antigen (PSMA) and is being evaluated for use in the evaluation of patients with known primary prostate cancer for metastatic involvement. The antibody is known to react with membrane-rich fractions of LNCaP cells, but not with soluble cytosol or secretary glycoproteins such as PSA or PAP. The phase II dosimetry studies reported herein were performed in 21 patients at three different institutions.

MATERIALS AND METHODS

Radiopharmaceutical

The data presented in this article are from three study sites: the University of Massachusetts Medical Center (UMMC: 5 patients), University of Washington Medical Center (UWMC: 11 patients) and the Iowa City Veterans Administration Medical center (ICVAH: 5 patients). These studies were conducted under protocols 356In14, 356In15 and 356In16. Each patient received an intravenous infusion of 0.5 mg of CYT356 (7E11-C5.3-GYK-DTPA) labeled with approximately 185 MBq (5 mCi) ^{111}In.

Received Jul. 13, 1995; revision accepted Feb. 7, 1996.

For correspondence or reprints contact: A.B. Brill, MD, PhD, Nuclear Medicine Department, University of Massachusetts Medical Center, 55 Lake Ave. No., Worcester, MA 01655.

The desired amount of $^{111}InCl_3$ was drawn up for each patient and buffered with sodium acetate before mixing in a shielded vial with the antibody. The preparation was kept for half an hour to achieve maximum labeling and then filtered with 0.22 μM Millex GV before administration. Labeling efficiency was typically over 90% as determined by ITLC. The total amount of radioactivity administered was determined by measuring the syringe activity in a dose calibrator before and after infusion.

Nuclear Data

The nuclear data for ^{111}In, ^{114}In and ^{114m}In are given in Table 1. These are based on the data of Weber et al. (*1*). Only the contributions from ^{114m}In and ^{111}In are included in our dose calculations since the levels of ^{113m}In and ^{115m}In were negligible contributors. We assumed that ^{114m}In represented 0.06% of the injected activity at time of administration, as the ^{111}In labeled agent was injected within 24 hr of its arrival from the manufacturer, which is more than two half lives before the end of expiration (at which time the maximum allowable level is 0.16%). In addition, we assume that the ^{114}In and ^{114m}In contaminants share the same biological kinetics as ^{111}In.

Biological Data

Sequential biodistribution studies (up to 7–10 days postinjection) were performed including measurements of blood (serum), whole-body retention and organ activity content (serum, liver, spleen, kidneys, testes and red marrow). The amount of activity excreted in urine was measured based on frequent urine collections the first day, and subsequent 24 hr urine collections. Whole-body counts were obtained at each session. Stool was not collected. Measurements were made using a quantitative conjugate emission imaging protocol along with transmission imaging and a thickness-dependent camera sensitivity calibration (*2*).

Data Analysis

The fraction of the injected dose in source organs for patients imaged at UMMC and ICVAH was analyzed at UMMC. Image data from UMMC and ICVAH were analyzed based on data recorded on optical disks from those sites. The UWMC data were received already analyzed for organ uptake. The optical disks were read on a Picker Odyssey computer and data transmitted across a local area network to a Macintosh IIcx and DIP Station (Jandel) image analysis software was used for drawing regions of interest (ROIs) about the specified source organs and background regions. ROIs for all regions were identified for each patient separately at an early imaging session. These were linked to each other, saved and used for all subsequent analyses. The activity in each source organ was calculated after subtraction of background from adjacent regions at each measurement time based on sensitivity and transmission correction factors for each of the cameras used in the study (*2*).

The source organs included in the study were: the liver, spleen, kidneys, testes, bone marrow, heart chamber, lungs, urinary bladder contents and the remainder of the body along with the GI tract organs, i.e., gall bladder contents, LLI, SI and ULI. The calculated

TABLE 1
Radionuclides Properties

Radionuclides	^{111}In				^{114}In				^{114m}In			
Physical half-life	2.83 d				71.9 sec				49.51 d			
Decay mode	EC				EC, β^+ (0.54%), β^- (99.46%)				IT (95%), EC, β^+ (4.3%)			
Principal radiation			Δ_i				Δ_i				Δ_i	
	E_i keV	n_i	rad g/ (μCi hr)	Gy kg/ (Bq s)	E_i keV	n_i	rad g/ (μCi hr)	Gy kg/ (Bq s)	E_i keV	n_i	rad g/ (μCi hr)	Gy kg/ (Bq s)
γ	171.3	0.902	0.329	2.48E-14	1300	0.0014	0.00388	2.92E-16	190.3	0.154	0.0625	4.69E-15
γ	245.3	0.94	0.491	3.70E-14					558.4	0.044	0.0522	3.92E-15
γ									725.2	0.043	0.0669	5.03E-15
x-ray	23–27	0.826	0.042	3.13E-15	23–27	0.00361	0.00018	1.37E-17	23–28	0.363	0.019	1.43E-15
Nonpenetrating			0.074	5.56E-15			1.65	1.24E-13			0.303	2.27E-14

activity in the GI tract organs was based on a compartmental model proposed by Stabin, described below (*3*). The total content of radioactivity in the bone marrow was estimated from measurements over L2 and L3 vertebrae multiplied by a factor (22.5) (*4*). This factor scales the sampled activity to total marrow content. The remainder of the body activity at each sampling period was considered to be 100% of the injected activity minus the sum of all activities otherwise accounted for in the measured source organs and activity lost in urine. The partition of plasma activity included an assignment of 10% of the plasma pool to the heart and lungs, respectively (*5*). Serum clearance and urine excretion data were established based on the counting of serum, urine samples and standards, and at the end of the collection period. Organ data were quantitated after correction for physical decay.

Since serum tracer content is the most reliably and accurately quantitated data, it was used as a forcing function to fit kinetic data collected from each of the measured organs (*6*). Using the CONSAM program (Berman et al.) (*7*), least squares best fit curves were obtained for serum using biexponential functions. Accordingly, activity in the liver, spleen, bone marrow and kidneys were obtained. The urine data were fit assuming 4.8-hr voiding intervals. The activity measured in each organ reflects tissue fixed plus circulating activity.

The area under the curve (AUC) was determined from the best fit curves and extrapolated to infinity. The only losses (besides stool and urine) were assumed to come from physical decay of the tracer. The residence times (AUC/injected activity) so obtained (blood plus fixed activity) for each patient were calculated and average values were computed separately for each site for ^{111}In and ^{114m}In. These values were entered into the MIRDOSE3 program (*8*) for each patient separately and calculations were made using the S factors for ^{111}In and ^{114m}In and the MIRD formalism (*9,10*). The S-factors used for ^{114m}In include dose contributions from ^{114}In, with which it is in equilibrium.

The testicular region was included in the field of view in planar images of the pelvis for four UMMC and three ICVAH patients. Since in some of the patients transmission data were either unavailable or unreliable due to variations in patient positioning, the geometric mean of testicular uptake was calculated assuming 2″ and 4″ attenuation. In three patients, uptake in the testes was calculated from whole-body images using a correction factor obtained from patients in whom both planar and whole-body images were available.

The temporal pattern of fecal excretion was estimated using a compartmental analysis method (*3*) for three UMMC patients (Patients 3, 4, 5). The model includes all measured source organs, rest of body and urine data, and was fit using CONSAM. The model assumed that the liver is connected to the GI tract with 30% leaving via the gallbladder, and the rest was excreted directly into the small intestine. The transit times of the material through the GI tract were based on ICRP data (*11*). Figure 1 shows the model used and Figure 2 shows the computer fit data (FIA, i.e., fraction of injected activity versus time) for a typical patient. The excreted material in each segment of the GI tract was calculated, and these values along with organ content data were entered into MIRDOSE 3 for subsequent analyses. The fraction of the liver activity that enters the small intestine directly and via the gall bladder was estimated to be 10.8% which was obtained from average GI tract activity distributions for all subjects included in this series.

RESULTS

Plasma clearance data for each of the UMMC patients are plotted in Figure 3. The derived parameters from the computer fit data are given in Table 2. There is a wide range of fast clearance components (50% CV) and the late clearance is slow, but well defined (19% CV).

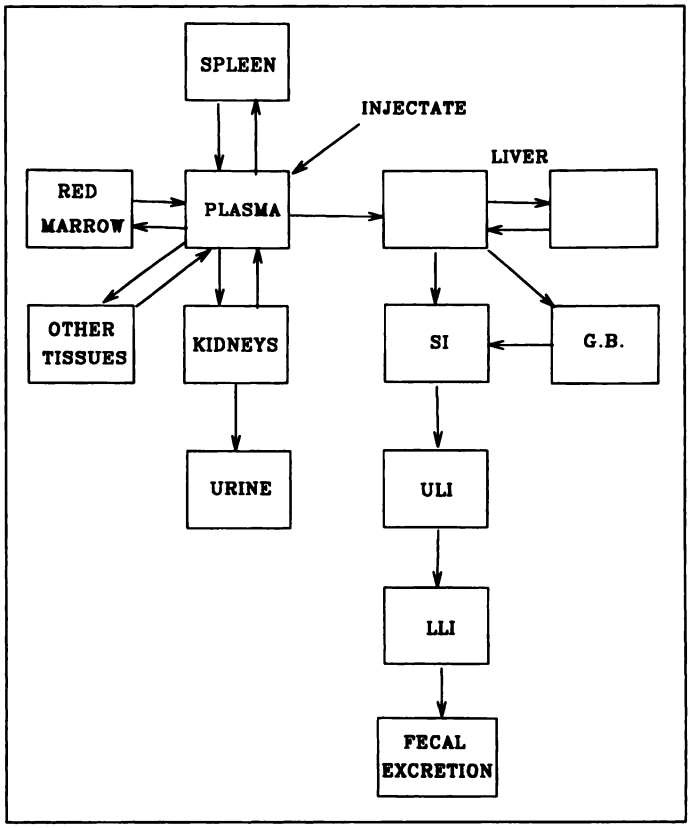

FIGURE 1. Compartmental model including GI tract.

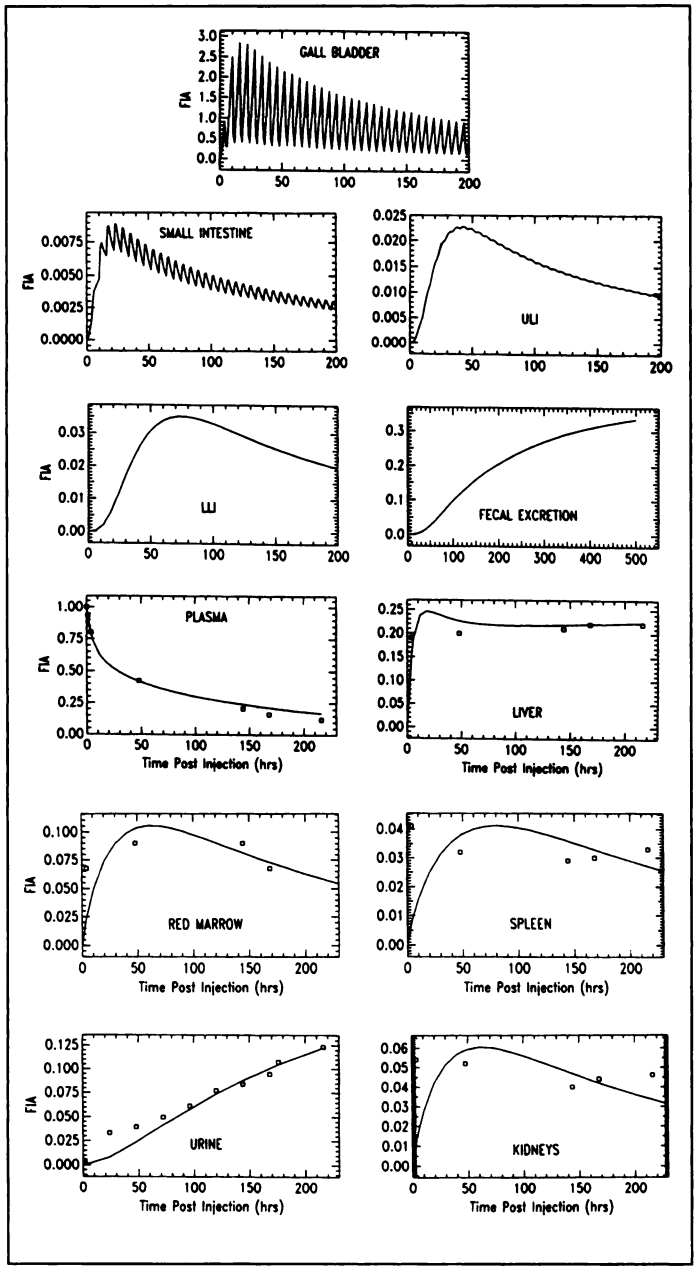

FIGURE 2. Observed data and computer best fit values (with GI tract model).

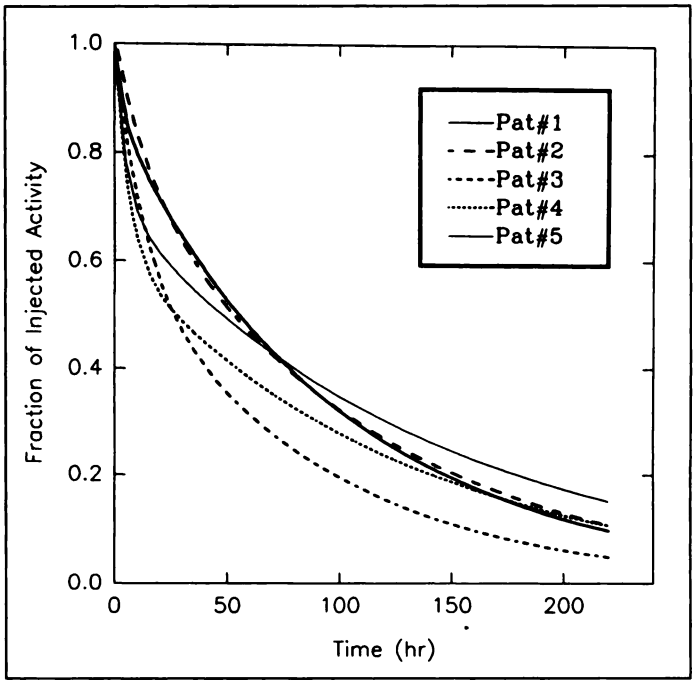

FIGURE 3. Pharmacokinetic data (University of Massachusetts Medical Center patients).

Table 3 presents the average values and s.d. of residence times for measured source organs (including GI tract activity and testicles). The liver has the highest residence time, while the kidney has the greatest intersite variation. No data were available from UWMC for the testes. Individual patient doses were calculated and the average values of dose to the different target organs are presented in Table 4 separately for each of the study centers. The effective dose (ED) was computed using ICRP 1990 weighting factors and is shown on the bottom line of Table 4 as essentially equal across study centers.

Fecal excretion was estimated to account ultimately for the loss of 27% of the injected activity with the remainder of the injected activity excreted in the urine. Table 5 presents the organ dose distribution calculated for the average of all patients with and without the GI excretory pathway. Inclusion of the GI tract increases the ED by 18%, as shown in the bottom row of Table 5.

DISCUSSION

These averaged dose estimates attempt to provide a measure of the overall risk associated with different procedures, despite the fact that the organs that receive the dose may be very different.

Dose estimates for the patients studied at the different institutions included in this study are in reasonable accord for individual organ doses within study sites, as well as between different sites. The greatest variation was seen in the dose administered to the kidneys (range 0.28–1.7 mGy/MBq) and dose administered to the testes, when considered as a source organ. There was a great variation in testicle dose between patients. In many patients, the testes are only barely visualized while in others the activity was clearly visualized. Testicular dose estimates ranged from 0.14–0.54 mGy/MBq. The inclusion of the testes as source organs increased the contribution to the ED from 0.21 to 0.25 mSv/MBq on average, i.e., by 16%. In addition to the testicular uptake per se, part of the increased dose is due to the relatively long blood residence time (45 hr versus 38 hr for OncoScint CR/OV) which contributes to increased dose to all organs. Despite the long radiological half-time of ^{114m}In, its contribution to the total dose is not large (3.5% of the total ED).

Excretion through the GI tract was modeled and 10.8% of the activity was assigned to the MIRDOSE3 excretory path. This corresponded to measured losses in patients who meticulously collected their urine. The use of the GI tract as a modeled source organ increased the dose to the lower large intestine by a factor of four.

CONCLUSION

The total-body absorbed dose from ^{111}In-Capromab Pendetide was found to be 0.14 mGy/MBq, and the effective dose is 0.25 mSv/MBq (including the testicle as a source organ). If one includes the dose from simulated transit through the GI tract, the ED dose is further increased by 18%. These dose estimates are similar in magnitude to the total-body and effective doses listed in the package insert for OncoScint CR/OV, 0.15 mGy/MBq and 0.23

TABLE 2
CYT-356 Pharmacokinetics—University of Massachusetts Medical Center Patients

Patient no.	β (hr)	α (hr)	AUC (mCi hr/ml)	CL (ml/hr)	MRT (hr)	V_{ini} (ml)	V_{ss} (ml)
1	99	3	0.237	22.2	141	2277	3134
2	69	3	0.232	22.8	99	1991	2266
3	76	9	0.220	24.7	106	2201	2617
4	59	8	0.142	36.6	80	2129	2931
5	87	4	0.199	27.2	122	2157	3310
Mean ± s.d.	78 ± 15	6 ± 3	0.206 ± 0.039	26.7 ± 5.9	110 ± 23	2151 ± 106	2852 ± 417

α = half-life of fast component; β = half-life of slow component; AUC = area under curve; CL = clearance; MRT = mean residence time; Vini = initial volume of distribution; Vss = steady state volume.

TABLE 3
Residence Times (hr) of CYT-356

	^{111}In				
Tissue	UWMC	UMMC	ICVAH	Average	s.d.
Plasma	47.46	39.60	43.89	44.73	5.63
Liver	22.21	32.87	28.31	26.20	9.14
Spleen	3.19	2.00	4.06	3.11	1.38
Red marrow	10.62	9.16	4.08	8.71	3.60
Kidneys	1.46	3.45	7.81	3.45	2.99
Blad. contents	0.31	0.30	0.26	0.29	0.13
Rem. body	38.53	21.95	27.34	31.92	10.20
Lungs	4.74	3.96	4.39	4.47	0.55
Heart chamber	4.74	3.96	4.39	4.47	0.55
Gall bladder		0.11		0.11	0.03
SI		0.42		0.42	0.11
ULI		1.19		1.19	0.32
LLI		1.76		1.76	0.47
Testes*		0.23–0.3	0.23–0.28	0.23–0.29	
	^{114m}In				
Plasma	0.301	0.154	0.140	0.227	0.097
Liver	0.103	0.082	0.264	0.136	0.151
Spleen	0.012	0.010	0.017	0.013	0.010
Red marrow	0.029	0.032	0.015	0.027	0.023
Kidneys	0.006	0.019	0.026	0.014	0.022
Blad. contents	0.0004	0.0000	0.0003	0.0003	0.0002
Rem. body	0.583	0.286	0.379	0.464	0.255
Lungs	0.030	0.020	0.010	0.023	0.010
Heart chamber	0.030	0.020	0.010	0.023	0.010
Gall bladder		0.0001		0.0001	0.0000
SI		0.0006		0.0006	0.0002
ULI		0.0020		0.0020	0.0008
LLI		0.0037		0.0037	0.0014
Testes*		0.002–0.003	0.002–0.003	0.002–0.003	

*For a range of transmission thickness (2"–4").

TABLE 4
Average Dose Estimates (mGy/MBq) Obtained from All Participating Sites

Target Organ	UMMC (n = 5)			UWMC (n = 11)			ICVAH (n = 5)		
	^{111}In	^{114m}In	Total	^{111}In	^{114m}In	Total	^{111}In	^{114m}In	Total
Adrenals	0.28	0.002	0.28 ± 0.05	0.26	0.005	0.26 ± 0.03	0.30	0.003	0.31 ± 0.04
Brain	0.04	0.002	0.04 ± 0.02	0.07	0.005	0.07 ± 0.01	0.04	0.003	0.05 ± 0.01
Gallbladder wall	0.39	0.002	0.39 ± 0.11	0.31	0.005	0.32 ± 0.05	0.37	0.004	0.38 ± 0.07
LLI wall	0.08	0.002	0.08 ± 0.02	0.11	0.005	0.11 ± 0.01	0.08	0.003	0.08 ± 0.01
Small intestine	0.12	0.002	0.12 ± 0.01	0.14	0.005	0.14 ± 0.01	0.12	0.003	0.13 ± 0.01
Stomach	0.14	0.002	0.14 ± 0.01	0.16	0.005	0.16 ± 0.02	0.16	0.003	0.17 ± 0.02
ULI wall	0.14	0.002	0.14 ± 0.01	0.15	0.005	0.15 ± 0.01	0.14	0.003	0.14 ± 0.02
Heart wall	0.37	0.010	0.38 ± 0.04	0.42	0.020	0.44 ± 0.03	0.40	0.010	0.41 ± 0.04
Kidneys	0.65	0.033	0.68 ± 0.32	0.37	0.011	0.38 ± 0.06	1.25	0.045	1.30 ± 0.33
Liver	1.18	0.023	1.20 ± 0.45	0.83	0.028	0.85 ± 0.19	1.04	0.072	1.11 ± 0.33
Lungs	0.28	0.008	0.28 ± 0.03	0.30	0.016	0.32 ± 0.02	0.29	0.007	0.30 ± 0.03
Muscle	0.08	0.002	0.09 ± 0.01	0.10	0.005	0.11 ± 0.01	0.09	0.003	0.10 ± 0.01
Pancreas	0.26	0.002	0.26 ± 0.04	0.26	0.005	0.26 ± 0.03	0.30	0.003	0.30 ± 0.04
Red marrow	0.22	0.003	0.22 ± 0.04	0.25	0.005	0.26 ± 0.04	0.16	0.003	0.16 ± 0.03
Bone surfaces	0.19	0.003	0.20 ± 0.02	0.24	0.005	0.24 ± 0.02	0.16	0.003	0.16 ± 0.02
Skin	0.05	0.002	0.05 ± 0.01	0.06	0.004	0.07 ± 0.00	0.05	0.003	0.05 ± 0.01
Spleen	0.57	0.028	0.60 ± 0.27	0.85	0.034	0.89 ± 0.31	1.09	0.048	1.14 ± 0.45
Testes	0.22	0.033	0.26	0.27	0.033	0.30	0.26	0.033	0.29
Thymus	0.12	0.002	0.12 ± 0.01	0.15	0.005	0.15 ± 0.01	0.12	0.003	0.13 ± 0.01
Thyroid	0.05	0.002	0.06 ± 0.02	0.08	0.005	0.09 ± 0.01	0.06	0.003	0.06 ± 0.01
Urine bladder wall	0.09	0.001	0.09 ± 0.02	0.11	0.003	0.12 ± 0.02	0.09	0.002	0.09 ± 0.01
Total body	0.13	0.003	0.13 ± 0.01	0.14	0.006	0.14 ± 0.01	0.13	0.005	0.14 ± 0.01
ED*	0.23	0.012	0.24 ± 0.02	0.25	0.014	0.27 ± 0.02	0.25	0.014	0.27 ± 0.02

*mSv/MBq.

TABLE 5
Comparison of Average Dose Estimates (mGy/MBq) without Including GI Tract as Source Organ

Target Organ	With GI source			Without GI source		
	^{111}In	^{114m}In	Total	^{111}In	^{114m}In	Total
Adrenals	0.28	0.004	0.28	0.28	0.004	0.28 ± 0.04
Brain	0.05	0.004	0.06	0.05	0.004	0.06 ± 0.02
Gallbladder wall	0.39	0.003	0.39	0.35	0.004	0.36 ± 0.08
LLI wall	0.40	0.009	0.41	0.09	0.004	0.10 ± 0.02
Small intestine	0.18	0.002	0.18	0.13	0.004	0.13 ± 0.01
Stomach	0.16	0.004	0.17	0.16	0.004	0.16 ± 0.02
ULI wall	0.27	0.004	0.27	0.14	0.004	0.15 ± 0.01
Heart wall	0.40	0.015	0.42	0.40	0.015	0.42 ± 0.04
Kidneys	0.65	0.024	0.67	0.64	0.024	0.67 ± 0.44
Liver	0.96	0.037	1.00	0.98	0.037	1.02 ± 0.32
Lungs	0.29	0.012	0.31	0.29	0.012	0.31 ± 0.03
Muscle	0.10	0.004	0.11	0.10	0.004	0.10 ± 0.01
Pancreas	0.27	0.004	0.27	0.27	0.004	0.27 ± 0.04
Red marrow	0.23	0.004	0.23	0.22	0.004	0.22 ± 0.05
Bone surfaces	0.21	0.004	0.22	0.21	0.004	0.21 ± 0.04
Skin	0.06	0.004	0.06	0.06	0.004	0.06 ± 0.01
Spleen	0.84	0.037	0.88	0.84	0.037	0.88 ± 0.37
Testes	0.27	0.033	0.30	0.26	0.033	0.30
Thymus	0.14	0.004	0.14	0.13	0.004	0.14 ± 0.02
Thyroid	0.07	0.004	0.08	0.07	0.004	0.07 ± 0.02
Urine bladder wall	0.12	0.002	0.12	0.10	0.002	0.10 ± 0.02
Total body	0.14	0.005	0.14	0.13	0.005	0.14 ± 0.01
ED*	0.28	0.014	0.29	0.24	0.013	0.25 ± 0.02

*mSv/MBq.

mSv/MBq, respectively, which is an agent approved for use in colorectal and ovarian cancer diagnosis and management.

NOTE ADDED IN PROOF

Since manuscript submission, the FDA requested an estimate of the dose to the prostate, which we estimated at 0.44 mGy/MBq based on the following assumptions: 0.01% uptake/g in a 16-g prostate with infinite retention. Reference data were taken from: Stabin M. A Model of the Prostate Gland for Use in Internal Dosimetry. *J Nucl Med* 1994;35: 516–520.

ACKNOWLEDGMENTS

We thank Cytogen Corp. for providing the antibody and for financial support.

REFERENCES

1. Weber DA, Eckerman KF, Dillman LT, Ryman JC. MIRD radionuclide data and decay schemes. New York: Society of Nuclear Medicine 1989.
2. Doherty P, Schwinger R, King M, Gionet M. Distribution and dosimetry of indium-111-labeled F(ab')2 fragments in humans. Fourth International Radiopharmaceutical Symposium, CONF-851113 (DE86010102) 1985;464–476.
3. Stabin MG. Prediction of radiation dose to the GI tract from analysis of blood and liver time-activity curves. In: *Fifth international radiopharmaceutical dosimetry symposium*. Oak Ridge Associated Universities, Oak Ridge, TN 1992;202–215.
4. Report on the Task Group on Reference Manual. ICRP Publication 23, Pergamon Press, 1974.
5. Poston JW, Aissi A, Hui TY, Jimba BM. A preliminary model of the circulating blood for use in radiation dose calculations. In: *Fourth international radiopharmaceutical dosimetry symposium*. Oak Ridge Associated Universities, Oak Ridge, TN 1985;574–586.
6. Kawaguchi EH. *The CONSAM User's Manual*. Research Facility for Kinetic Analysis, Seattle, WA 1990.
7. Berman M, Beltz WF, Greif PC, Chabay R, Boston RC. CONSAM User's Guide. Laboratory of Mathematical Biology, National Institutes of Health, Bethesda, MD 1983.
8. Stabin MG. MIRDOSE: Personel computer software for internal dose assessment in nuclear medicine. *J Nucl Med* 1996;37:538–546.
9. Watson EE. The MIRD Internal Dose Formalism. Chapter 15. In: *Internal radiation dosimetry*. O.G. Raabe, ed. Health Physics Society 1994 Summer School. Madison, WI: Medical Physics Publishing Co., 1994.
10. Loevinger R, Berman M. A revised schema for calculating the absorbed dose from biologically distributed radionuclides. MIRD Pamphlet No 1 (Revised). New York: The Society of Nuclear Medicine, 1976.
11. Eckerman K. Chapter 13 Dosimetric Methodology of the ICRP. In: *Internal radiation dosimetry*. O.G. Raabe, ed. Health Physics Society 1994 Summer School. Madison, WI: Medical Physics Publishing, 1994.

(continued from page 9A)

FIRST IMPRESSIONS:

Persistent Back Pain in a Case of Breast and Lung Cancer

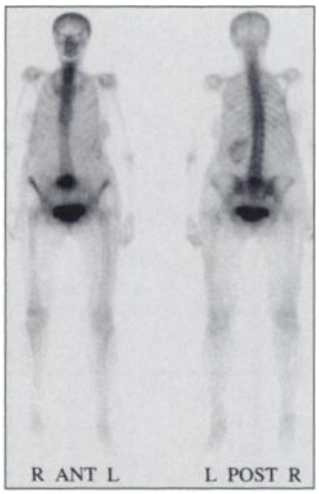

Figure 1.

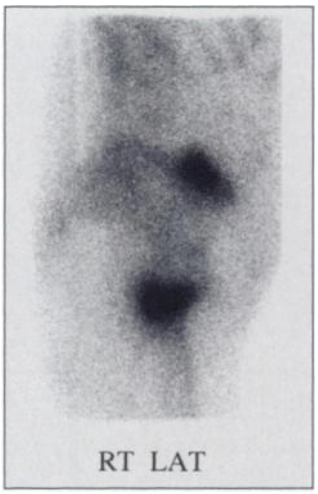

Figure 2.

Figure 3.

PURPOSE

A 74-yr-old woman with a history of breast and lung carcinoma presented with persistent back pain. Planar whole-body images showed a focus of markedly increased tracer uptake in the region of the S1 vertebra, which was more intense on the anterior image. The left kidney was normally located; the right kidney was not visualized (Fig. 1). These scintigraphic observations resulted in obtaining a right lateral spot view (Fig. 2), which depicted intense tracer uptake anterior to the sacrum, suggestive of ptotic right kidney with marked stasis. The lumbrosacral spine was normal. An IVP study (Fig.3), performed 4 mo before whole-body imaging, showed a ptotic right kidney. On the IVP study, the kidney's position is more medial. This case illustrates the importance of awareness of alternative causes of abnormal tracer uptake, especially when routine images are atypical.

TRACER

Technetium-99m-MDP

ROUTE OF ADMINISTRATION

Intravenous

TIME AFTER INJECTION

Three hours

INSTRUMENTATION

Dual-head Genesys (ADAC) gamma camera

CONTRIBUTORS

A. El-Shirbiny, M. Imbriaco, H. Yeung, J.J. Zhang and C. Divgi, Memorial-Sloan Kettering Cancer Center, New York, NY.